INTERNATIONAL ATOMIC ENERGY AGENCY
UNITED NATIONS EDUCATIONAL, SCIENTIFIC AND CULTURAL ORGANIZATION
INTERNATIONAL CENTRE FOR THEORETICAL PHYSICS
I.C.T.P., P.O. BOX 586, 34100 TRIESTE, ITALY, CABLE CENTRATOM TRIESTE

SMR.764 -8

RESEARCH WORKSHOP ON CONDENSED MATTER PHYSICS
13 JUNE - 19 AUGUST 1994

WORKING GROUP ON
"DISORDERED ALLOYS"
8 - 19 AUGUST 1994

"Application of TB-LMTO for ground state structural stability of binary intermetallics"

PART II

G. P. DAS, A. ARYA and S. BANERJEE
Solid State Physics Division
B.A.R.C. Bombay 400085
INDIA

---

1. INTRODUCTION

There is a growing interest in combining microscopic electronic structure with statistical mechanics to arrive at a first principles description of intermetallic phase stability [1–3]. The idea is to get the *configurational energy* corresponding to a certain alloy configuration by utilizing some suitable electronic structure total energy calculations (which can take into account the many-body interactions) and then, to include the finite temperature effects, by incorporating the *configurational entropy* contribution via cluster variation method (CVM) based on mean field approximation of the Ising model. For theoretical investigation of the ground state structural stability of a substitutional alloy, one needs to know the configurationally averaged effective cluster interactions (ECI's), which can be obtained either starting from the ordered state or from the disordered state [4,5]. Accordingly, there are two extreme approaches to do averaging over various clusters or configurations viz. (a) the Connolly-Williams method (CWM) [6] which starts from some selected ordered ground state structures and (b) augmented space recursion technique [7,8] in real space for averaging over *all possible* disordered configurations. The standard CPA based approaches [2,9], and the method of direct configuration averaging (DCA) [3,10], as well as their intercomparison [11] have been amply discussed in the literature.

The success of the Connolly-Williams type cluster expansion depends on the rapid convergence of the volume dependent (but concentration independent) ECI's with cluster size [12]. Once the ECI's are known for a given binary intermetallic system, the energies of disordered and ordered states may be computed on an equal footing. In this process one gets the relative stabilities of the ordered equilibrium (stable) phases as well as of the various possible metastable phases which are difficult to probe experimentally. It is also possible to extract free energies of the disordered terminal solid solutions as a function of solute concentration. An essential prerequisite for the abovementioned approach for extraction of ECI's is to have a reliable and efficient electronic structure method for calculation of the total energies of the ordered ground state superstructures of a binary intermetallic. Within the framework of Hohenberg-Kohn-Sham density functional theory (DFT) [13] and the widely accepted local density approximation (LDA) [14,15], the electronic structure of crystalline solids can be most efficiently handled

using the linear band structure methods, introduced by Andersen[16,17]. The linear muffin-tin orbital (LMTO) method, when used within atomic sphere approximation (ASA), is particularly attractive for handling complex systems, because of the ease with which the structure dependent part and the potential dependent part are separated out in the secular equation [16,18,19]. An important milestone is the realization ten years ago [20], that the original infinite ranged LMTO basis set can be transformed exactly into new basis sets which are *localized* in real space. This so-called tight-binding (TB-) LMTO method has the computational simplicity of the empirical tight-binding schemes, as well as the accuracy characteristic of a first principles method. Apart from providing a localized basis with its obvious application potentials, the TB-LMTO method also yields the full nonspherical charge density needed for accurate total energy and force calculations [21,22].

Extensive experimental investigations have been carried out on the Li-Al system, which exhibits a number of fcc and bcc based ground state superstructures (both stable and metastable) in the entire concentration range of the phase diagram [23]. From the application point of view, the metastable $\delta - Al_3Li$ phase is an important constituent of a low density, high strength-to-weight, damage tolerant alloy, used for weight critical applications in the aircraft industry [24]. From fundamental point of view, the Li-Al intermetallics belong to a relatively simple family *without* any $d-$electrons, and interesting variations in the nature of chemical bonding are manifested with change of structure and/or composition.

In a previous paper [25], we had discussed the stability analysis of fcc-based ground state superstructures of Li-Al alloys, in the first nearest neighbour (NN) pair interactions. Here we have extended the calculations to include the second NN interactions also. The Li-Al alloy system is incoherent one, because of the fact that the pure constituents have different crystal lattices. Accordingly, both fcc and bcc based superstructures (fig. 1) have been taken into account, scanning the entire concentration range, e.g. we have considered A_3B (AB_3), A_2B (AB_2) and AB stoichiometries. The justifications for extending the calculations to higher nearest neighbours are (a) going up in the hierarchy of cluster approximation improves the level of approximation, on which the calculations (viz. CWM and CVM) are based; and (b) a larger number of structures can be incorporated in the analysis giving rise to a more representative stability profile. We have deployed the

TB-LMTO-ASA method for a systematic investigation, at zero temperature, of various ordered Li-Al intermetallics which are possible candidates under the above approximation. The plan of the paper is as follows. Section 2 gives the essential points related to our present electronic structure computation. In section 3 we summarize our results on electronic and cohesive properties and the method of extraction of ECI's using CWM. Finally, we summarize our main findings in section 4.

2. COMPUTATIONAL DETAILS

As mentioned above, we have used here LMTO-ASA method for electronic structure calculations, the details of which are given in the original papers and reviews by Andersen and his coworkers [16–22]. The self-consistent potentials are generated by solving the scalar relativistic Schrödinger equation [32] along with the von Barth-Hedin LDA parametrization [14] of the exchange-correlation potential. This LMTO-ASA method is ideally suited for the relatively close packed intermetallic structures treated here, where one can ensure reasonably small overlap between the atomic spheres without introducing any interstitial ('Empty') spheres. In LMTO-ASA, the approximation due to spherical averaging is managable, provided the overlap between the spheres, defined as $[(s_1 + s_2 - d) * 100/s_1]$ is less than 30%; here s_1 and s_2 $(s_1 \leq s_2)$ are the radii of the two overlapping spheres and d is the distance between them. Incorporating the so-called 'combined correction', one can partly salvage the error due to spheridization of potential and charge density. This has been calculated here by following a method based on the energy derivative of the screened structure constant matrix [21,26] . We have used the *same* Wigner-Seitz radius (S_{av}) for Al and Li in a given structure, even though, strictly speaking one should adjust the sphere radii (conserving the cell volume of course) which will ensure their approximate charge neutrality [27]. The LMTO-ASA method has the advantage of using the same type of (minimal) basis set for all the elements in the periodic table. The computer program used for the present calculations [26] has already been deployed for self-consistent calculations for $s-$, $p-$, $d-$ and $f-$electron elements, and the corresponding potential parameters have been tabulated [22,28]. In our calculation, although $s-$, $p-$ and $d-$partial waves have been used (i.e. maximum angular momentum l_{max}=2), the

d–orbitals on both Li and Al sites have been *downfolded* [26]. It is worth noting at this point that we can not afford to eliminate the d–orbitals altogether from the basis set expansion, because of the anisotropic bonding between the Al atoms strengthened by the fractional valence electrons donated by Li. Restricting the basis set to l_{max}=1 might lead to wrong trend in cohesive and elastic properties [29,30]. That is why we have retained l_{max}=2 but *downfolded* the d–orbitals of Li, thereby restricting the size of the Hamiltonian and overlap matrices, but without sacrificing the accuray of our results. This is a unique feature of the present TB-LMTO-ASA method [20,26]. Finally, the tetrahedron method for Brillouin zone (i.e. k-space) integrations has been used with its latest version, which avoids misweighting and corrects errors due to the linear approximation of the bands inside each tetrahedron [31]. 15 equispaced k-points have been chosen along each direction of the cubic Brillouin Zone, resulting in *converged* k-mesh. Knowing the ASA potentials, the ground state charge densities can be calculated quite accurately and hence the ASA total energies of the various ordered configurations [32].

3. RESULTS AND DISCUSSION

A. Stability of ground state superstructures of Li-Al

We have considered 11 fcc-based and 6 bcc-based ground state ordered superstructures with A_3B, A_2B, AB, AB_2 and AB_3 stoichiometries under first and second nearest neighbour interactions only i.e. by taking octahedron-tetrahedron cluster approximation for fcc lattice and irregular tetrahedron cluster approximation for bcc lattice. All the crystallographic information needed for self-consistent TB-LMTO-ASA calculations on each of these structures (fig. 1) are summarized in table 1. We have minimized the total ground state energy as a function of the unit cell volume. All the calculated ground state properties (see table 2) correspond to the respective equilibrium volumes, both for fcc- and bcc-based structures. These are the equilibrium lattice constant a_0 (or equivalently the average Wigner-Seitz radius S_{av}), the bulk modulus B, the cohesive energy E_{coh} and the compound formation energy E_{form}, all tabulated as a function of Li-concentration or equivalently the (valence-shell) electron to atom ratio (e/a). The S_{av} values plotted as a function of Li-concentration (Fig. 2) shows some kind

of a parabolic trend with minimum at equiatomic Li-Al. The decrease in S_{av} with the addition of Li (in Al-rich alloys) was also obtained from earlier calculations [27,29] and is in direct contradiction with Vegard's law. In the Li-rich side, however, S_{av} again starts increasing steadily with Li-concentration. Our calculated S_{av} values and hence the equilibrium lattice constants, which are $\sim$ 1% smaller than the experimental values, wherever available (see table 2). The error is largest in case bcc-Li, where the lattice constant is 3% larger than that experimentally obtained. Taking into account the zero-point motion and the effect of thermal expansion, the discrepancy may slightly narrow down, but this underestimate is mainly attributed to the use of LDA.

The bulk modulus $B=(C_{11}+2C_{12})/3$, which is related to the curvature of the total energy as $B(V)=VE''(V)$, has been calculated for each structure and composition; it is found to decrease monotonically with increasing Li-concentration (Fig. 3). Our bulk moduli values are in very good agreement with experiment; in fact, the earlier LAPW calculations [30,33] showed bigger discrepancies with experimental values. First principles calculations of shear moduli (C_{11}-C_{12} and C_{44}), poisson's ratio (σ) and Young's modulus $E=3B(1-2\sigma)$ are however more cumbersome as they require computation of total energy as a function of symmetry lowering lattice strains [33,34], which is beyond the scope of our present ASA calculation.

By subtracting from the ASA total energy of the compound, the sum total of the energies of the atomic constituents weighted by their respective fractional concentrations, we get the cohesive energy. The free-atom calculations have been performed semi-relativistically with a large cutoff (r_{max}=30a.u.). Our calculated E_{coh} values are found to increase with decreasing Li-concentration i.e. with increasing e/a ratio (see table 2 and fig. 4). The systematic overestimate of the absolute values of E_{coh} compared to experimental values is attributed partly to our atomic calculation [25] and partly to the shape approximation used in ASA.

Even though our cohesive energies are overestimated, the error involoved (i.e. ΔE_{coh}) is clearly systematic and therefore gets more or less cancelled in the calculation of energy of formation. For example, E_{form} (see table 2) is minimum for AlLi in the B32 structure making it the most stable compound, and our calculated value (-26.29 kJ/mol) is in very good agreement with the thermochemical data (-24.30 kJ/mol)[35]. Fig. 5 depicts the variation of the calculated formation energies, which lie within a V-

shaped boundary, in close conformity with the LAPW predictions [1]. While calculating the formation energies of the fcc-based compounds, we have taken fcc-Al and fcc-Li as our reference systems, whose ground state total energies (in fact their weighted sum) have been subtracted to calculate the corresponding formation energies. For bcc-based compounds, similarly, we have taken the bcc-Al and bcc-Li total energies as the reference. The two points in fig. 5 (and table 2) for the bcc-Al and bcc-Li have been obtained by subtracting the corresponding total energies for the fcc-phases.

B. ECI's for Li-Al alloys

We have used Connolly-Williams prescription [6] for the calculation of effective cluster (multisite) interactions which are configuration as well as concentration independent, but are dependent upon the unit cell volume. By expanding the cohesive energies, obtained as a function of volume, around the equilibrium volume, V_0, and retaining terms upto second order, we get volume dependence of ECI's as

$$J_\gamma(V) = J_\gamma^{(0)} + J_\gamma^{(1)} V + J_\gamma^{(2)} V^2 \qquad (1)$$

Volume dependent ECI's for Li-Al system, based upon fcc and bcc parent lattices, have been determined by taking upto second NN pair approximation. Table 3(a) and 3(b) summarize the calculated coefficients for volume expansion ($J_\gamma^{(k)}$, k=0,1,2) of ECI for fcc and bcc lattices. These ECI's (J_γ), which are averaged over a number of candidate ground state superstructures, converge rather fast with increasing size of the cluster γ. As a cross-check on the reliability of these configurationally averaged ECI's we have inserted these J_γ's, back into the original CWM expression and got back cohesive energy values of these superstructures, in close agreement with those obtained from our LDA calculations. This establishes the feasibility of using the TB-LMTO method, in conjunction with CWM for obtaining ECI's.

C. Electronic structure and chemical bonding

For $L1_0$, $L1_2$ and B32 phases of Li-Al alloy system, we had reported [25] the results of our self-consistent electronic structure calculations viz. total and partial densities of states (DOS), band structure, various potential

parameters etc. We had also discussed the subtle differences in chemical bonding as we change the Li concentration keeping the underlying lattice same (say fcc) and also when we change the structure (say from $L1_0$ to B32) keeping the composition fixed. In the present work, for the sake of brevity, we shall mention only the salient features of our results on the electronic structures of 11 fcc- and 6 bcc-based ground state superstructures without explicitly giving the DOS and bands. A few of these structures have been studied before using mainly LAPW method [30,33] and the corresponding DOS's and bands obtained from our TB-LMTO calculation are in reasonably good agreement with those results.

One interesting quantity is the fractional $l-$decomposed charge distribution (Q_l) in Al- and Li-spheres, as embedded in a given fcc or bcc based structure (see table 4(a) and 4(b)) whose total valence charge is anyway known. Since these quantities generated from our ASA calculation represent charges within the overlapping atomic spheres, these should not be directly used to explain the inter-site charge transfer. For example, the 'tail' of the Al-orbital protrudes into the neighbouring Li-sphere, whose size has been chosen to be same as that of the Al-sphere (and hence is relatively large). This results in a significant Al-like contribution to the Li-sphere charge, which is found to increase with increasing Al concentration. However, since we have used the *same* WS sphere radii around both Al and Li sites, it should be possible to estimate the intra-site promotion of electrons and also the relative trend in the *inter-site* (or more appropriately *inter-sphere*) charge transfer. For example, if we compare the Q_l for *AlLi* in $L1_0$ and B32 structures (see tables 4(a) and 4(b)), we observe that more charge is transferred from Li to Al sphere in the B32 structure; and it is this extra charge ($\sim$ 0.133 electrons) which goes in between the Al-bonds, resulting in a strengthening of Al-Al bonds in B32 structure. In other compounds, this inter-sphere charge transfers are much less. The intra-atomic charge redistribution (mainly promotion from $s-$like to $p-$like character) in both the Li and Al sites, can be observed in all the compounds, and is again most prominent in the B32 : *AlLi*, followed by that in $L1_2$: Al_3Li. These are, incidentally, the two most stable/metastable ordered structures which have been realized.

The DOS at Fermi level, $N(E_F)$, is another important quantity, as it is used for estimation of electronic specific heat, electron-phonon coupling

constant and even for determining the vibrational contribution to the entropy at finite temperature. These are also tabulated in Table 4. Amongst the stable (or metastable) lithium-aluminium intermetallics which are of interest, $N(E_F)$ is found to be minimum (1.971) for the AlLi in B32 structure, and maximum (5.269) for $AlLi_3$ in DO_3 structure, while the corresponding value for Al_3Li in $L1_2$ structure is intermediate (4.167). These numbers reflect the trend in metallicity in these ordered compounds.

4. SUMMARY

In this paper, we have reported the results of our first principles investigation of the zero temperature structural stability of a series of ordered binary compounds $Al_{1-c}Li_c$ spanning the entire concentration range $0 \leq c \leq 1$. We have considered 11 fcc based and 6 bcc based ground state superstructures, by restricting ourselves to the second NN pair approximation, within the mean field description of the Ising model. The self-consistent TB-LMTO-ASA method used here for total energy calculations, is an efficient first principles tool, which yields reasonably accurate cohesive properties matching with the available experimental results. The cohesive energies of all these superstructure not only show the correct stability sequence, but also can be used in conjunction with the Connolly-Williams prescription to yield the ECI's for a fixed lattice (say fcc or bcc). These ECI's can, in turn, be used to arrive at the configuration energy of a binary alloy, for both ordered and disordered alloys. In particular, for Li-Al system, which does not have large off-diagonal disorder, the ECI's are found to be converging rather fast, which is an essential requirement for the success of the CWM. In summary, our analysis reveals that the TB-LMTO-CWM is a viable approach to determine the energetics of a class of binary alloys.

Acknowledgment

This work forms a part of the Ph.D. project, carried out at Indian Institute of Technology, Bombay, by one of the authors (AA), who is thankful to Prof. M.J. Patni for his guidance and encouragement.

References

1 M. Sluiter, D. de Fontaine, X.Q. Guo, R. Podloucky and A.J. Freeman, Phys. Rev. **B 42**, 10460 (1990).

2 F. Ducastelle in *Order and phase stability in alloys*, North-Holland: New York, (1991)

3 C. Wolverton, G. Ceder, D. de Fontaine and H. Dreysse, Phys. Rev. **B 48**, 726 (1993).

4 F. Ducastelle and F. Gautier, J. Phys. **F6**, 2039 (1976)

5 M. Sluiter and P.E.A. Turchi, Phys. Rev. **B40**, 11215 (1989)

6 W. Connolly and A.R. Williams, Phys. Rev. **B 27** 5169 (1983); and in *The electronic structure of complex systems*, eds. W. Temmerman and P. Phariseau, (Plenum Press, New York, 1984) p. 581.

7 A. Mookerjee, in *Methods of Electronic Structure Calculations*, ed. O.K. Andersen, V. Kumar and A. Mookerjee (World Scientific, 1994).

8 T. Saha, I. Dasgupta and A. Mookerjee, J. Phys.: Cond. Matt. **6**, L245 (1994).

9 A. Gonis, M. Sluiter, P.E.A.Turchi, G.M. Stocks and D.M. Nicholson, J. Less Common Met. **168**, 127 (1991).

10 H. Dreysse, A. Berera, L. T. Wille and D. de Fontaine, Phys. Rev. **B39**, 2442 (1989)

11 A. Berera, Phys. Rev. **B 42**, 4311 (1990).

12 J. Mikalopas, P. A. Sterne, M. Sluiter and P. E. A. Turchi, in *High-Temperature Ordered Intermetallic Alloys IV*, eds. L. A. Johnson, D. P. Pope and J. O. Stiegler, MRS, Vol 213, 119 (1991)

13 P. Hohenberg and W. Kohn, Phys. Rev. **136**, B864 (1964); W. Kohn and L.J. Sham, Phys. Rev. **140**, A1133 (1965).

14 U. von Barth and L. Hedin, J. Phys. **C5**, 1629 (1972)

15 R.O. Jones and O. Gunnarsson, Rev. Mod. Phys. **61**, 689 (1989).

16 O.K. Andersen, Phys. Rev. **B12**, 3060 (1975).

17 O.K. Andersen, in *The Electronic Structure of Complex Systems*, ed. P. Phariseau and W.M. Temmerman (Plenum, New York, 1984), p. 11.

18 H.L. Skriver, *The LMTO Method* (Springer, Heidelberg, 1984).

19 O.K. Andersen, O. Jepsen and D. Glötzel, in *Highlights in condensed matter theory*, ed. F. Bassani, F. Fumi and M.P. Tosi (North Holland, Amstardem, 1985), p.59.

20 O.K. Andersen and O. Jepsen, Phys. Rev. Lett. **53**, (1984), 2571.

21 O. K. Andersen, in *Electronic band structure and its applications*, vol 283 of *Lecture Notes in Physics* ed. M. Yussouf, Springer, Berlin, (1987)

22 O.K. Andersen, in *Methods of Electronic Structure Calculations*, ed. O.K. Andersen, V. Kumar and A. Mookerjee (World Scientific, 1994).

23 A.J. McAlister, Bull. Alloy Phase Diagr. **3**, 177 (1982).

24 M. S. Yu and H. Chen, in *Kinetics of Ordering Transformation in Metals*, eds. H. Chen and V. K. Vasudevan, (The Minerals, Metals and Materials Society, 1992) p.307.

25 A. Arya, G.P. Das, H.G. Salunke and S. Banerjee, J. Phys.: Cond. Matt. **6**, 3389 (1994).

26 M. van Schilfgaarde, A.T. Paxton, O. Jepsen and O.K. Andersen, unpublished.

27 P.P. Singh and A. Gonis, Phys. Rev. **B 49**, 1642 (1994).

28 A. E. Kumm, Ph.D. Dissertation, University of Stuttgart (1992), unpublished.

29 K.I. Masuda-Jindo and K. Terakura, Phys. Rev. **B 39**, 7509 (1989).

30 X.Q. Guo, R. Podloucky, J. Xu and A.J. Freeman, Phys. Rev. **B 41**, 12432 (1990).

31 P. Blöchl, O.K. Andersen and O. Jepsen, Phys. Rev. **B** (1994), to appear.

32 O.K. Andersen, Z. Pawlowska and O. Jepsen, Phys. Rev. **B 34**, 5253 (1986).

33 M.M. Mehl, Phys. Rev. **B 47**, 2493 (1993).

34 M. Methfessel, Phys. Rev. **B 38**, 1537 (1988).

35 I. Barin, O. Knacke and O. Kubaschweski in *Thermochemical Properties of Inorganic Substances*, (Springer Verlag, Berlin,1977).

Table 1 : Crystallographic data for various fcc- and bcc- based superstructures upto second nearest-neighbour interactions. The numbers given in brackets against each space group are the corresponding space group numbers, and the Wyckoff positions, as cited in *International Table of Crystallography*.

fcc-based structures	Compositional formulae	Space Group symbol (no.)	Position of atoms	Multiplicity
A1	A	Fm3m (225)	A (a)	4
$L1_2$	A_3B	Pm3m (221)	A (c) B (a)	3 1
$L1_0$	AB	P4/mmm (123)	A (a) B (d)	1 1
$L1_1$	AB	R$\bar{3}$m (166)	A (a) B (b)	1 1
A_2B_2 type	A_2B_2	$I4_1$/amd (141)	A (a) B (b)	4 4
A_2B type	A_2B	Immm (71)	A (i) B (a)	4 2
DO_{22}	A_3B	I4/mmm (139)	A (d) A (b) B (a)	4 2 2
bcc-based structures				
A2	A	Im$\bar{3}$m (225)	A (a)	2
B2	AB	Pm$\bar{3}$m (221)	A (a) B (b)	1 1
B32	AB	Fd$\bar{3}$m (227)	A (a) B (b)	8 8
DO_3	A_3B	Fm$\bar{3}$m (225)	A (c) A (b) B (a)	8 4 4

Table 2 : Table of calculated ground state properties of fcc and bcc based Li-Al supersturctures. Quantities within brackets are the available experimental numbers.

fcc-based structures	e/a	S_{av} (a.u.)	Bulk modulus (GPa)	E_{coh} (kJ/mol)	E_{form} (kJ/mol)
Al (fcc)	3.0	2.954 (2.99)	76.797 (76.3)	-405.798	0.0
Al_3Li ($L1_2$)	2.5	2.947 (2.95)	68.934 (66.0)	-366.150	-9.896
Al_3Li (DO_{22})	2.5	2.945	65.631	-365.453	-9.199
Al_2Li	2.33	2.947	68.622	-347.150	-7.410
AlLi ($L1_0$)	2.0	2.922	61.572	-318.191	-11.479
Al_2Li_2	2.0	2.919	44.359	-318.021	-11.310
AlLi ($L1_1$)	2.0	2.952	44.378	-314.622	-7.911
$AlLi_2$	1.66	2.946	34.960	-283.400	-9.717
$AlLi_3$ ($L1_2$)	1.5	3.005	30.805	-261.589	-4.421
$AlLi_3$ (DO_{22})	1.5	2.957	29.319	-265.579	-8.411
Li (fcc)	1.0	3.107 (3.24)	19.033	-207.624	0.0
bcc-based structures					
Al (bcc)	3.0	2.982	94.501	-400.787	5.011
Al_3Li (DO_3)	2.5	2.950	61.290	-360.861	-8.574
AlLi (B2)	2.0	2.876	60.003	-322.715	-18.927
AlLi (B32)	2.0	2.915 (2.96)	78.959	-330.079	-26.290
$AlLi_3$ (DO_3)	1.5	2.942	33.336	-268.559	-13.270
Li (bcc)	1.0	3.136 (3.24)	12.021 (12.0)	-206.789	0.835

Table 3(a) : Effective (multisite) interaction coefficients ($J_\gamma^{(k)}$) for bcc lattice under tetrahedron approximation. Successive clusters ($\gamma = 0$, 1, .., 5) correspond, respectively, to empty (0), point (1), nn pair (2), nnn pair (3), triangle containing one nnn pair (4) and tetrahedron (5). Units for calculation of J_γ is kJ/mol [see text].

γ	$J_\gamma^{(o)}$	$J_\gamma^{(1)}$	$J_\gamma^{(2)}$
0	-46.64	-57.55	3.05
1	72.83	-34.60	1.78
2	10.40	3.37	-0.36
3	-40.34	11.16	-0.63
4	29.78	-6.64	0.34
5	41.67	-10.24	0.58

Table 3(b) : Effective (multisite) interaction coefficients ($J_\gamma^{(k)}$) for fcc lattice under octahedron-tetrahedron approximation. Successive clusters γ =0,1,..,10 correspond, respectively, to empty (0), point (1), nn pair (2), nnn pair (3), eqililateral nn triangle (4), 2nn-1nnn isosceles triangle (5), equililateral tetrahedron (6), 5nn-1nnn irregular tetrahedron (7), 4nn square (8), pyramid (9) and octahedron (10). Units for calculation of J_γ is kJ/mol [see text].

γ	$J_\gamma^{(o)}$	$J_\gamma^{(1)}$	$J_\gamma^{(2)}$
0	-86.78	-48.09	2.53
1	81.90	-36.78	1.91
2	7.12	0.92	-0.10
3	-4.36	0.95	-0.05
4	-17.98	4.62	-0.26
5	-57.97	9.27	-0.41
6	15.41	-4.14	0.26
7	-35.32	9.32	-0.56
8	16.02	-3.18	0.16
9	26.32	-6.00	0.34
10	19.42	-3.70	0.18

Table 4(a) : Number of valence electrons (Q_l) inside the atomic (WS) spheres, partitioned according to angular momentum, for fcc based superstructures. Q_{sph}'s are nothing but the fractional number of electrons inside the Al and the Li spheres, as embedded in the respective compounds. Weighted sum of these sphere charges yields the total valence charge in the compound.

STRUCTURE	Al				Li				Total valence charge	$N(E_F)$ States/ Ry.atom
	Q_s	Q_p	Q_d	Q_{sph}	Q_s	Q_p	Q_d	Q_{sph}		
Al (fcc)	1.104	1.476	0.420	3.0	-	-	-	-	3	4.187
Al_3Li ($L1_2$)	1.118	1.444	0.268	2.830	0.421	0.832	0.257	1.510	10	4.167
Al_3Li (DO_{22})	1.126 1.125	1.400 1.438	0.290 0.268	2.816 2.830	0.430 -	0.851 -	0.242 -	1.522 -	10	4.117
Al_2Li	1.130	1.406	0.250	2.786	0.441	0.797	0.189	1.427	7	5.134
AlLi ($L1_0$)	1.130	1.344	0.151	2.624	0.424	0.802	0.150	1.376	8	4.267
AlLi ($L1_1$)	1.150	1.385	0.223	2.758	0.402	0.725	0.115	1.242	4	1.459
Al_2Li_2	1.116	1.359	0.158	2.633	0.423	0.797	0.148	1.368	8	6.026
$AlLi_2$	1.156	1.320	0.101	2.577	0.431	0.679	0.101	1.211	5	4.396
$AlLi_3$ ($L1_2$)	1.231	1.213	0.064	2.508	0.451	0.631	0.082	1.164	6	5.953
$AlLi_3$ (DO_{22})	1.179 -	1.263 -	0.054 -	2.500 -	0.445 0.433	0.655 0.618	0.082 0.090	1.182 1.140	6	5.108
Li (fcc)	-	-	-	-	0.492	0.478	0.031	1	1	6.634

Table 4(b) : Same as table 4 (a) for bcc based superstructures.

STRUCTURE	Al				Li				Total valence charge	$N(E_F)$ States/ Ry.atom
	Q_s	Q_p	Q_d	Q_{sph}	Q_s	Q_p	Q_d	Q_{sph}		
Al (bcc)	1.153	1.437	0.410	3.0	-	-	-	-	3	5.040
Al_3Li (DO_3)	1.117 1.151	1.484 1.364	0.364 0.255	2.965 2.770	0.444 -	0.804 -	0.247 -	1.500 -	10	5.025
AlLi (B2)	1.084	1.249	0.128	2.461	0.445	0.912	0.182	1.539	4	2.736
AlLi (B32)	1.067	1.541	0.151	2.759	0.378	0.707	0.156	1.241	8	1.971
$AlLi_3$ (DO_3)	1.165 -	1.246 -	0.051 -	2.461 -	0.395 0.459	0.568 0.710	0.067 0.085	1.031 1.254	6	5.269
Li (bcc)	-	-	-	-	0.498	0.471	0.031	1	1	6.599

Figure Captions

18

Fig. 1 : Crystal structures of some of the fcc and bcc based ordered intermetallic phases ($L1_1$, A_2B, A_2B_2, DO_{22} *and* $B2$ etc.). Remaining structures like $L1_2$, $L1_0$ *and* $B32$ have been dealt with in ref [25].

Fig. 2 :Average Wigner-Seitz radii of ordered Li-Al compounds as a function of Li-concetration (filled and open circles correspond, respectively, to bcc and fcc based superstructures). The continuous curve has been drawn to indicate the trend in equilibrium volume per atom with concentration.

Fig. 3 : Calculated bulk moduli for various Li-Al compounds (in the same notation as in fig 2).

Fig. 4 : Calculated cohesive energies of Li-Al compounds as a function of the valence electron/atom ratio (in the same notation as in fig. 2).

Fig. 5 : Calculated energies of formation of Li-Al compounds as a function of Li-concentration (in the same notation as in fig 2). See text for details.

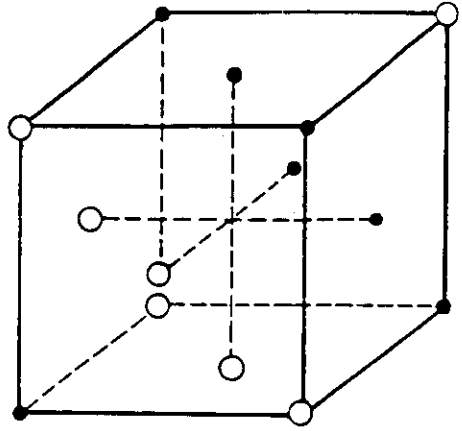

$L1_1$ STRUCTURE

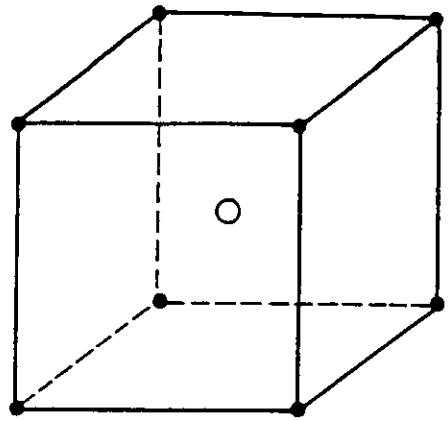

B2 STRUCTURE

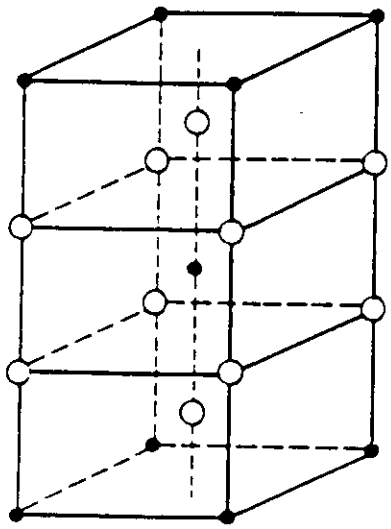

A_2B STRUCTURE

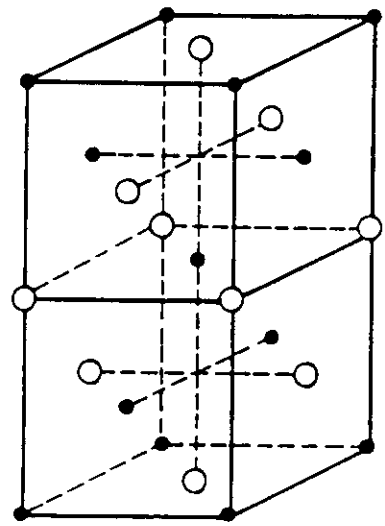

A_2B_2 STRUCTURE

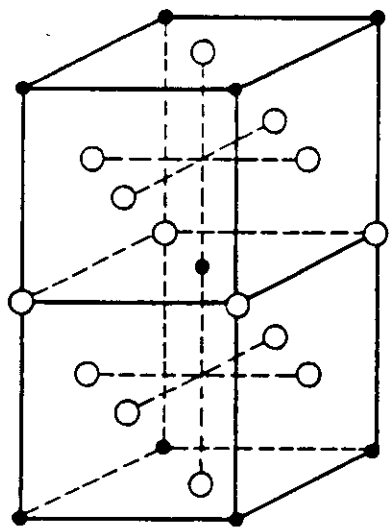

DO_{22} STRUCTURE

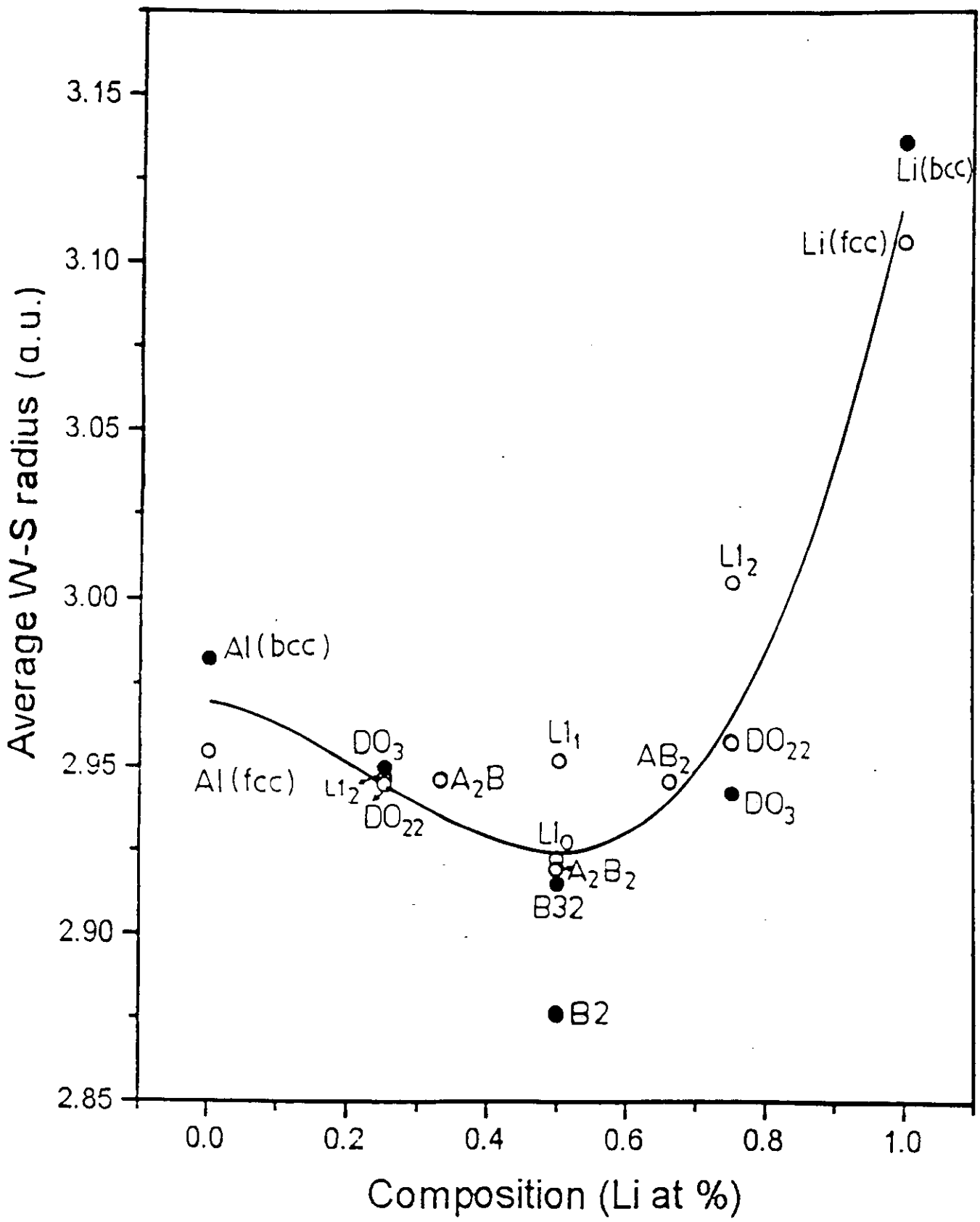
Average W-S radius (a.u.)
3.15
3.10
3.05
3.00
2.95
2.90
2.85
0.0
0.2
0.4
0.6
0.8
1.0
Composition (Li at %)
Li(bcc)
Li(fcc)
$L1_2$
Al(bcc)
Al(fcc)
DO_3
$L1_2$
DO_{22}
A_2B
$L1_1$
AB_2
DO_{22}
DO_3
$L1_0$
A_2B_2
B32
B2

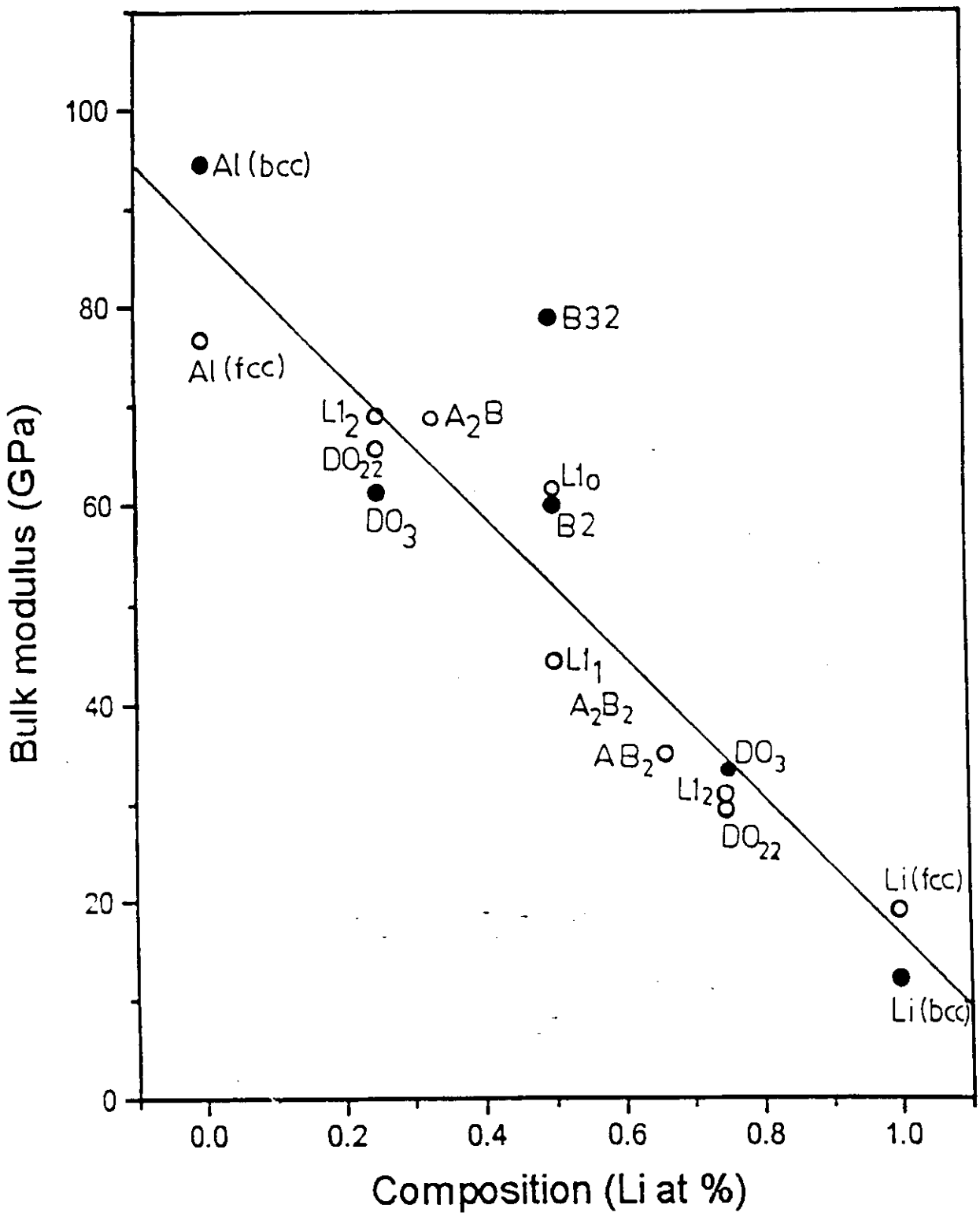
Bulk modulus (GPa)
Composition (Li at %)
100
80
60
40
20
0
0.0
0.2
0.4
0.6
0.8
1.0
Al (bcc)
Al (fcc)
B32
L1$_2$
A$_2$B
DO$_{22}$
DO$_3$
L1$_0$
B2
L1$_1$
A$_2$B$_2$
AB$_2$
DO$_3$
L1$_2$
DO$_{22}$
Li (fcc)
Li (bcc)

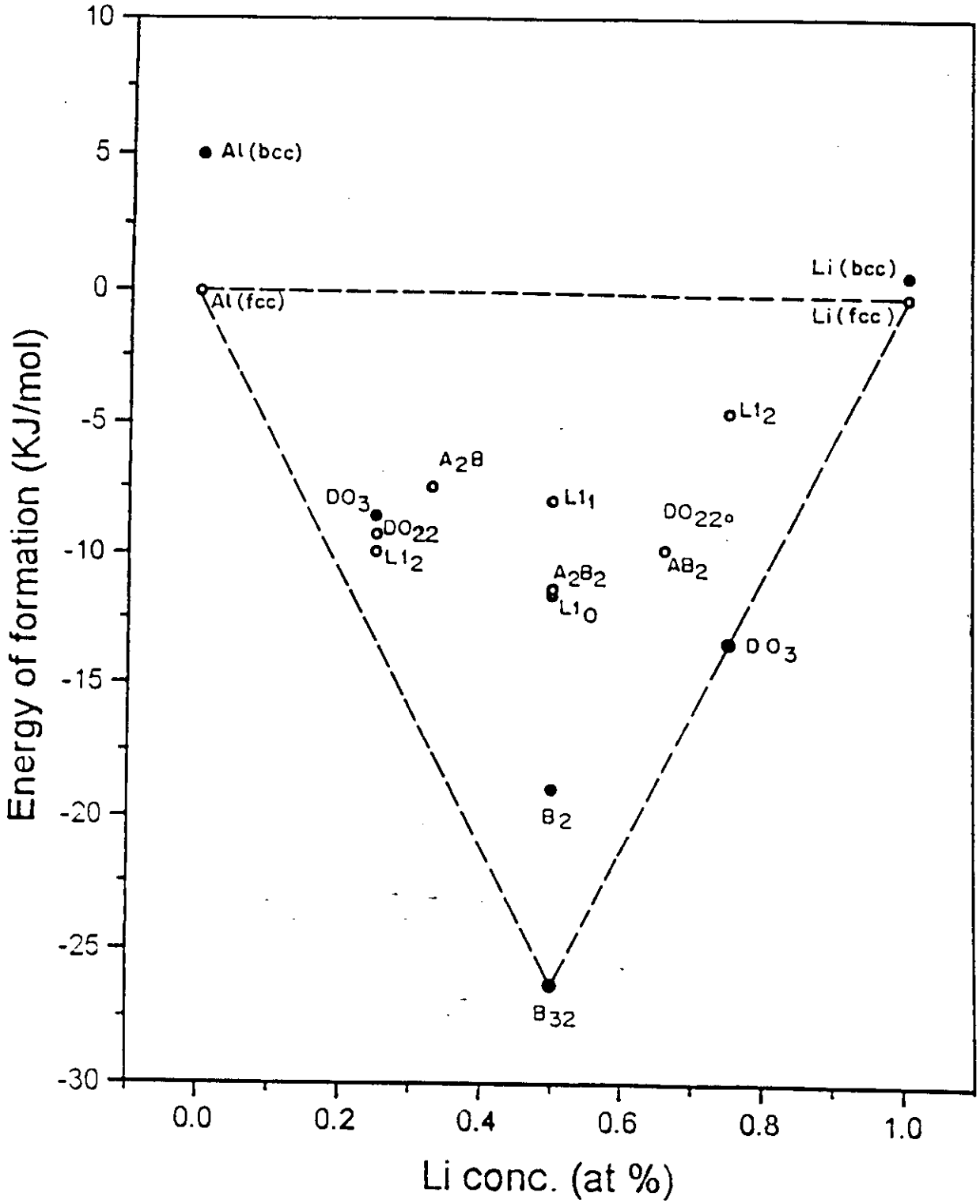
Energy of formation (KJ/mol)
Li conc. (at %)
10
5
0
-5
-10
-15
-20
-25
-30
0.0
0.2
0.4
0.6
0.8
1.0
Al (bcc)
Al (fcc)
Li (bcc)
Li (fcc)
A2B
DO3
DO22
L12
L11
DO22
AB2
A2B2
L10
DO3
B2
B32

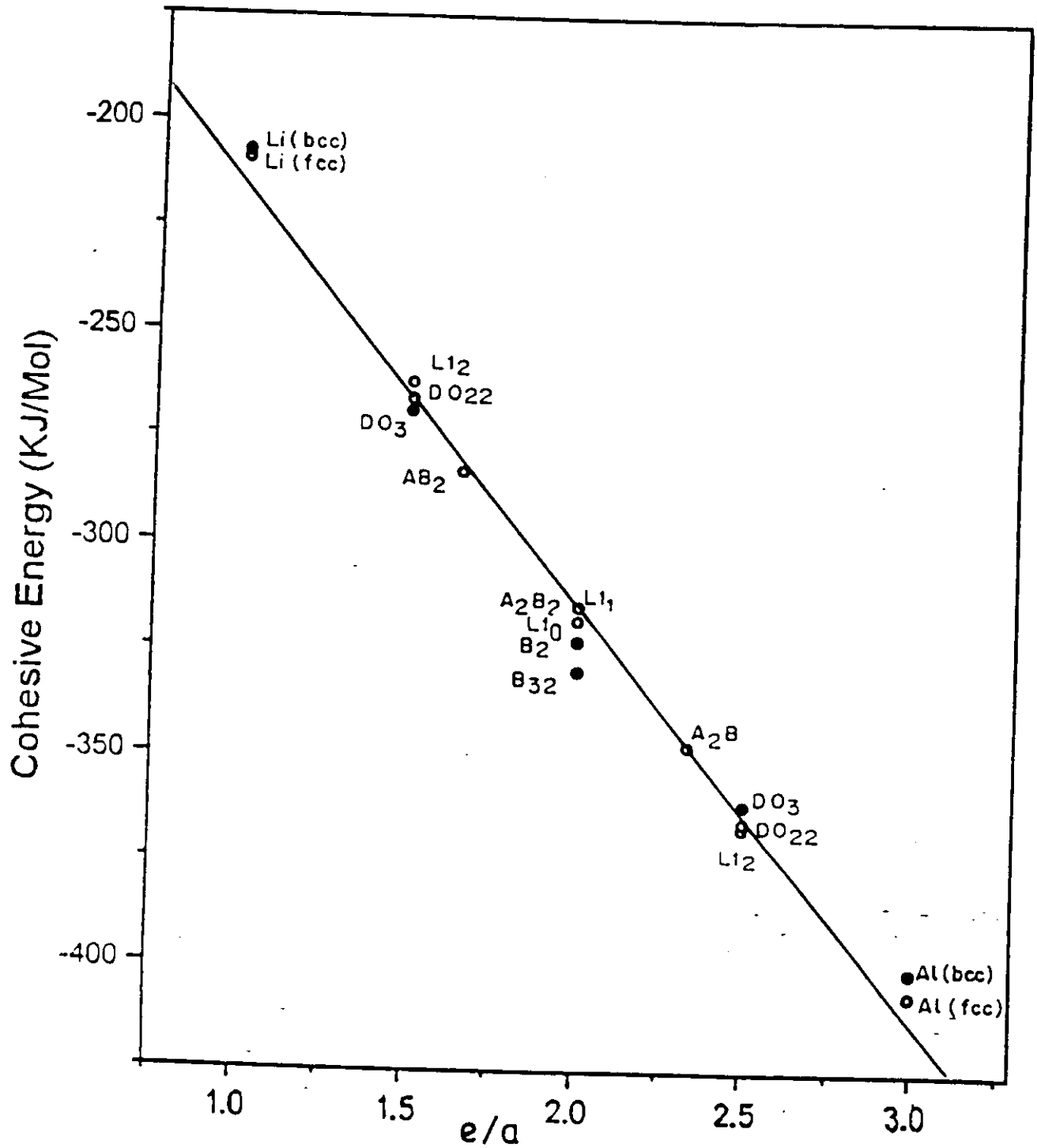
Cohesive Energy (KJ/Mol)
-200
-250
-300
-350
-400
1.0
1.5
2.0
2.5
3.0
e/a
Li (bcc)
Li (fcc)
L12
D022
DO3
AB2
A2B2
L11
L10
B2
B32
A2B
DO3
D022
L12
Al (bcc)
Al (fcc)